Heliyon 11 (2025) e41635

Contents lists available at ScienceDirect

Heliyon

journal homepage: www.cell.com/heliyon

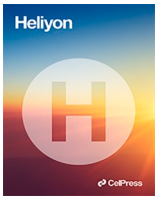

Research article

Clusterin induced by OPC phagocytosis blocks IL-9 secretion to inhibit myelination in a model of Alzheimer's disease

Rebecca M. Beiter [a,b,c,**,1], Tula P. Raghavan [a,b,d,1], Olivia Suchocki [a,b], Hannah E. Ennerfelt [a,b], Courtney R. Rivet-Noor [a,b], Andrea R. Merchak [a,b], Jennifer L. Phillips [e,f,g], Tim Bathe [e,f,g], John R. Lukens [a,b], Stefan Prokop [e,f,g], Jeffrey L. Dupree [h], Alban Gaultier [a,b,*]

[a] Center for Brain Immunology and Glia, Department of Neuroscience, Charlottesville, VA 22908, USA
[b] Graduate Program in Neuroscience, Charlottesville, VA 22908, USA
[c] Department of Neurobiology, UMass Chan Medical School, Worcester, MA 01655, USA
[d] Medical Scientist Training Program, University of Virginia School of Medicine, Charlottesville, VA 22908, USA
[e] Center for Translational Research in Neurodegenerative Disease, College of Medicine, University of Florida, Gainesville, FL, 32610, USA
[f] Department of Pathology, College of Medicine, University of Florida, Gainesville, 32610, USA
[g] McKnight Brain Institute, College of Medicine, University of Florida, Gainesville, FL, 32610, USA
[h] Department of Anatomy and Neurobiology, Virginia Commonwealth University, Richmond, VA 23298, USA

ARTICLE INFO

Keywords:
Oligodendrocyte progenitor cells
Astrocyte
Clusterin
Myelin
Alzheimer's disease
IL-9

ABSTRACT

Background: Variants in the *CLUSTERIN* gene have been identified as a risk factor for late-onset Alzheimer's disease and are linked to decreased white matter integrity in healthy adults. However, the specific role for clusterin in myelin maintenance in the context of Alzheimer's disease remains unclear.
Methods: We employed a combination of immunofluorescence and transmission electron microscopy techniques, primary culture of OPCs, and an animal model of Alzheimer's disease.
Results: We found that phagocytosis of debris such as amyloid beta, myelin, and apoptotic cells, increases clusterin expression in oligodendrocyte progenitors. We further discovered that exposure to clusterin inhibits differentiation of oligodendrocyte progenitors. Mechanistically, clusterin blunts production of IL-9 and addition of exogenous IL-9 can rescue clusterin-inhibited myelination. Lastly, we demonstrate that clusterin deletion in mice prevents myelin loss in the 5XFAD model.
Discussion: Our data suggest that clusterin could play a key role in Alzheimer's disease myelin pathology.

1. Introduction

Alzheimer's Disease (AD) is a neurodegenerative disease with limited therapeutic options to effectively prevent disease

* Corresponding author. Center for Brain Immunology and Glia, Department of Neuroscience, Charlottesville, VA 22908, USA.
** Corresponding author. Center for Brain Immunology and Glia, Department of Neuroscience, Charlottesville, VA 22908, USA.
E-mail addresses: Rebecca.Beiter@umassmed.edu (R.M. Beiter), ag7h@virginia.edu (A. Gaultier).
[1] These authors contributed equally.

https://doi.org/10.1016/j.heliyon.2025.e41635
Received 22 July 2024; Received in revised form 1 January 2025; Accepted 1 January 2025
Available online 3 January 2025

progression, and patients inevitably succumb to debilitating dementia [2]. White matter loss has been documented in AD patients, but how this myelin loss contributes to disease progression is not completely understood [52]. Recent studies indicate that generation of new myelin-forming oligodendrocytes is critical for memory consolidation and recall [49,57]. Additionally, remyelination therapeutics have been shown to reduce cognitive deficits seen in an animal model of AD [14]. This evidence supports the hypothesis that inability to generate oligodendrocytes and maintain myelin could be a significant driver of the cognitive deficits observed in AD.

The adult brain contains oligodendrocyte progenitor cells (OPCs), a highly proliferative population of glia that are maintained in a progenitor state throughout adulthood and are normally capable of generating nascent oligodendrocytes [17,33]. However, in AD, OPCs fail to repair myelin damage for yet unknown reasons. The ability of OPCs to produce mature, myelinating oligodendrocytes during adulthood is critical, as motor learning, memory consolidation, and memory recall are all dependent on the *de novo* production of myelin [41,49,57].

Clusterin, also known as apolipoprotein J, is a glycoprotein widely expressed in the brain, where it plays roles in neurodegeneration, apoptosis, and inflammation [43]. It helps prevent the aggregation of misfolded proteins like amyloid-beta, offering neuroprotective effects. However, it also influences immune responses and apoptosis, contributing to both protective and pathological processes in diseases like Alzheimer's, where elevated clusterin levels are associated with disease progression [22,39,62,71]. Single nucleotide polymorphisms (SNPs) in human *CLUSTERIN* gene are known risk factors for AD development [6,37]. Besides expression in astrocytes, we have recently documented through single cell transcriptomic analysis of the adult mouse brain that a subset of OPCs express *Clusterin* [5]. Here, we investigated if clusterin alters the function of OPCs in AD [28]. We found that OPCs in both normal aging individuals and Alzheimer's patients express clusterin, in agreement with single-cell sequencing data [26]. These data indicate that, in addition to astrocytes, OPCs also increase clusterin expression in the context of AD [26]. Consequently, we investigated what factors might contribute to clusterin production in OPCs. We found that phagocytosis of debris such as oligomeric Aβ and myelin debris results in upregulation of clusterin production by OPCs. We further discovered that soluble clusterin acts a potent inhibitor of OPC differentiation and prevents production of myelin proteins *in vitro*. At a mechanistic level, we found that clusterin suppresses OPC secretion of interleukin-9 (IL-9), and that adding back exogenous IL-9 during OPC culture can rescue differentiation and myelination in the presence of clusterin. Deletion of clusterin *in vivo* improved myelination in the 5XFAD mouse model of AD, supporting the role of clusterin in inhibition of myelination. Collectively, these results suggest that clusterin could be a new therapeutic target in efforts to enhance remyelination in neurodegenerative diseases like AD and multiple sclerosis.

2. Material and methods

2.1. Animals

C57BL/6J (Jackson, #000664) were purchased from Jackson or bred at the University of Virginia. 5xFAD mice (Jackson #34848) were bred at the University of Virginia [47]. Clusterin knockout mice (Jackson #005642) were bred at the University of Virginia. Mice were maintained on a 12-h light/dark cycle with lights on at 7am. All animal experiments were approved and complied with regulations of the Institutional Animal Care and Use Committee at the University of Virginia (protocol #3918). All experiments were conducted and reported according to ARRIVE guidelines (https://arriveguidelines.org/arrive-guidelines).

2.2. Human tissue samples

Research involving human participants was conducted in accordance with the Code of Ethics of the World Medical Association (Declaration of Helsinki). Postmortem brain tissues were obtained from the University of Florida Human Brain and Tissue Bank with approval from the University of Florida Institutional Review Board (IRB201600067). All patients or their next-of-kin provided informed consent for brain donation. Clinical details of all human specimens analyzed are provided in Supplemental Table 1.

2.3. OPC and astrocyte culture

OPCs were cultured as previously described, with a few modifications [50]. Briefly, postnatal cortices (P0-P4) were rapidly dissected, and meninges removed. The tissue was digested in 2 ml of Accutase (Gibco, A1110501) supplemented with 50 units/mL DNase (Worthington Biochemical, LS002139). Cells were then passed through a 70 μm filter and grown in suspension in neurosphere media consisting of DMEM/F12 (Gibco, 11320082), B27 (Gibco, 17504044), Pen-Strep (Gibco, 15140122), and 10 ng/mL EGF (Peprotech, 315–09). Following expansion as neurospheres, cells were switched to oligosphere media consisting of DMEM/F12 (Gibco, 11320082), B27 (Gibco, 17504044), Pen-Strep (Gibco, 15140122), 10 ng/mL FGF (Peprotech, 450–33), and 10 ng/mL PDGF-AA (Peprotech, 315–17). Cells were allowed to grow in suspension for at least 2 days. Cells were then plated as attached OPCs on 0.01 % Poly-L-Lysine coated plates (Electron Microscopy Sciences, 19320-B) in the same media. Cells were allowed to attach for at least 12 h and then subsequent assays were performed. Astrocytes were prepared as previously described [24]. Astrocytes were switched to serum free media for 3 h before adding clusterin or vehicle.

2.4. OPC proliferation

OPCs were plated in proliferation media (described above) supplemented with 8 μg/mL clusterin (Sino Biological 50485-M08H) or an equivalent volume of vehicle (H_20 or PBS) for the control samples. OPCs were allowed to proliferate for 40–72 h. Cell number was

assessed using the Cell Counting Kit-8 (Dojindo, CK04) according to manufacturer's instructions. Optical density (OD) was measured at 450 nm. For data analysis, the OD of a media only control was subtracted from the OD of all experimental samples. The OD of wells treated with clusterin were then normalized to the biologically identical control well.

2.5. OPC differentiation

OPCs were plated in proliferation media (described above) or differentiation media consisting of DMEM/F12 (Gibco, 11320082), B27 (Gibco, 17504044), Pen-Strep (Gibco, 15140122), 10 ng/mL FGF (Peprotech, 450–33), 10 ng/mL CNTF (Peprotech, 450–13), and 40 ng/mL T3 (Sigma, T6397). For clusterin conditions, 8 μg/mL clusterin (Sino Biological 50485-M08H) was added to the differentiation media and an equivalent volume of vehicle (H_20 or PBS) was added to the differentiation and proliferation control samples. For IL-9 rescue experiments, 100 ng/ml IL-9 (Peprotech 219–19) was added to the differentiation media and an equivalent volume of vehicle (0.1 % BSA) was added to the differentiation and proliferation control samples. For VEGF inhibition experiments, 10 μg/ml of a VEGF function-blocking antibody (R&D Systems MAB9947-SP) was added to differentiation media and 10 μg/ml of control IgG (Biolegend 403501) was added to the differentiation and proliferation control samples. OPCs were allowed to differentiate for 48–72 h and were then subsequently processed for RNA extraction and qPCR or for immunofluorescence.

2.6. Aβ preparation and in vitro treatment

Aβ oligomers were prepared as previously described [58]. Briefly, human Amyloid $Beta_{1\text{-}42}$ (Echelon Biosciences, 641–15) was dissolved in HFIP (Sigma, 52517) to make a 1 mM solution and was allowed to desiccate overnight. The resulting peptide film was diluted to a 5 mM solution in DMSO and subsequently diluted to a 100 μM solution in phenol-free F-12 cell culture media (Gibco, 11039–021) and allowed to incubate overnight at 4 °C. For the analysis of clusterin expression following Aβ-treatment, OPCs were treated with 3 μM Aβ or a vehicle control for 4 h 3 μM Aβ was chosen as it is within the typical range of Aβ treatment for primary cultures of brain-resident cells and did not cause overt cell death [11,46,60]. For experiments that included samples treated with CytoD, cells were pretreated for 30 min with 1 μM CytoD (Millipore-Sigma, C8273) or DMSO and subsequently treated with 3 μM Aβ or vehicle control (also containing CytoD or DMSO) for 4 h. For astrocyte cell were switched to serum free media during the Aβ-treatment. For CypHer-labeled Aβ experiments, 400 μM Aβ oligomers in DMSO and phenol-free F-12 cell culture media was incubated with an equivalent volume of 0.1M sodium bicarbonate (Fisher Scientific, S233-500) and 400 μM CypHer5e (Cytiva, PA15401) for 30 min at room temperature. Following incubation, the solution was spun through a buffer exchange column (Thermo Scientific, 89882) to remove any excess dye.

2.7. Myelin preparation and in vitro treatment

Myelin was prepared from mouse brains as previously described [24]. Purified myelin was passed through an insulin syringe prior to use to ensure cells were treated with a homogenous solution. Cells were treated with 100 μg/ml myelin or vehicle control for 4 h. For two replicates that included samples treated with CytoD, cells were pretreated for 30 min with 1 μM CytoD (Millipore-Sigma, C8273) or DMSO and subsequently treated with 100 μg/ml myelin or vehicle control (also containing CytoD or DMSO) for 4 h. For the remaining two replicates that included samples treated with CytoD, no pretreatment was performed. Pretreatment with CytoD did not alter clusterin expression when compared to no pretreatment with CytoD, so all experiments were combined and plotted in Fig. 2F. Cells treated with myelin were washed once with PBS prior to RNA preparation.

2.8. Cytokine and H_20_2 in vitro treatment

OPCs were treated with 10 ng/ml TNFα, 10 ng/ml IFNγ, 10 μM H_20_2 or the relevant control for 3 h and then processed for qPCR.

2.9. ELISA

OPCs were grown as described above. A 10 cm dish of approximately 2 million OPCs was treated with 3 μM Aβ or an equivalent volume of vehicle for 72 h. Cells were lysed for 15 min in RIPA buffer (PBS, 1 % Triton X-100, 0.5 % deoxycholic acid, 1 % sodium dodecyl sulfate) supplemented with 1× protease inhibitor (MedChem Express HY-K0010). The insoluble material was removed by spinning the lysate at 15,000g for 15 min. The resulting lysate was used to quantify the amount of clusterin present in each sample using the Mouse Clusterin ELISA Kit (Thermo Fisher EM18RB) according to manufacturer's instructions.

2.10. Luminex Assay

OPCs were grown as described above. Cells were treated with 8 μg/ml clusterin for 24 h (1 replicate) or 72 h (1 replicate). Media was then collected and spun to remove all cellular debris. Media was concentrated using a 3KD cutoff concentrator column (Thermo Fisher 88526). The resulting concentrate was analyzed using the Milliplex 32-plex Mouse Cytokine/Chemokine Panel (Millipore Sigma MCYTMAG-70K-Px32) according to manufacturer's instructions.

2.11. Apoptotic cell preparation and in vitro treatment

To create apoptotic cells, Jurkats were treated with 150 mJ of UV energy and incubated for 2–4 h at 37 °C in complete media consisting of RPMI 1640 Media (Gibco, 11875101), 10 % FBS (R&D Systems, S12450H), and Pen-Strep (Gibco, 15140122). Apoptotic cells were washed and added to cultured OPCs at approximately a 1:1 ratio for 6 h. OPCs were washed once prior to RNA isolation.

2.12. Aβ injections

C57BL/6J mice (8–14 weeks) were injected with 1 μl of CypHer-Aβ (1 mg/ml, ipsilateral) and NHS-Fluorescein (contralateral, Thermo Fisher 46410) as previously described [51]. Briefly, mice were anesthetized with a mixture of ketamine and xylazine and a small burr hole was drilled in the skull. 1 μL of 100 μM Aβ was injected at a speed of 200 nL/min into the right hemisphere. 1 μL of 200 μM NHS-Fluorescein diluted in PBS was injected into the left hemisphere at the same speed. Injections were targeted for 2 mM lateral, 0 mM anterior, and −1.5 mM deep relative to bregma. Mice were given ketoprofen following surgery and were euthanized 12 h post-injection.

2.13. Immunofluorescence and electron microscopy

Mice were deeply anesthetized with pentobarbitol and subsequently perfused with 5 units/mL heparin in saline followed by 10 % buffered formalin, each for approximately 1 min. For brain tissue, brains were rapidly dissected and post-fixed in 10 % buffered formalin overnight at 4 °C. Tissue was then transferred into 30 % sucrose in PBS and allowed to sink for at least 24 h. Brains were frozen in OCT, sectioned, and stored in PBS plus 0.02 % NaAz until further staining.

Tissue or cultured cells were blocked with PBS, 1 % BSA, 0.5 % Triton-X 100, 2 % normal donkey serum, and 1:200 CD16/CD32 (14-0161-82, 1:200, eBioscience) for at least 1 h at room temperature. For stains utilizing a mouse primary antibody, tissue was blocked in Mouse-on-Mouse Blocking Reagent (MKB-2213, Vector Laboratories) according to manufacturer's instructions for at least 1 h at room temperature. Samples were incubated in primary antibodies overnight at 4 °C with gentle agitation. Samples were then washed three times in TBS containing 0.3 % Triton-X 100 and incubated in secondary antibodies overnight at 4 °C with gentle agitation. Following secondary incubation, samples were stained with Hoechst (1:700, ThermoFisher Scientific, H3570) for 10 min at room temperature, washed three times in TBS containing 0.3 % Triton-X 100, and mounted on slides using Aqua Mount Slide Mounting Media (Lerner Laboratories). Images were collected on a Leica TCS SP8 confocal microscope and processed using Fiji.

For quantitative ultrastructural analysis, mice were deeply anesthetized and transcardially perfused with 0.9 % NaCl followed by a Millonig's buffer solution (pH 7.3) containing 5 % glutaraldehyde and 4 % paraformaldehyde. Following the post-fixation, brains were harvested, vibratome sectioned and processed for standard electron microscopic analysis as previously described [23]. Briefly sagittal brain sections, containing the corpus callosum at the level of the fornix, were fixed in 1 % cacodylate buffered osmium tetroxide, dehydrated in graded ice-cold ethanol and embedded in PolyBed 812 embedding resin (Polysciences, Inc., Fort Washington, PA). Ultrathin (70 nm) sections were stained with uranyl acetate and lead citrate and imaged using a JEOL JEM 1400Plus transmission electron microscope (JEOL, Peabody, MA) equipped with a Gatan OneView CMOS camera (Gatan Inc., Pleasanton, CA). Electron micrographs were collected at 10,000×; a minimum of 100 myelinated axons per mouse were used to calculate g-ratios.

2.14. Antibodies for immunofluorescence

Primary antibodies used for immunofluorescence were PDGFRα (1:200, R&D Systems, AF1062), Olig2 (1:200, Millipore, MABN50), Clusterin (1:250, Abcam, AB184100), MBP (1:500, Abcam, ab7349) and Aβ (1:300, Cell Signaling Technology, 8243S). Secondary antibodies used were Donkey anti-Goat Cy3 (2 μg/mL, Jackson ImmunoResearch, 705-165-147), Donkey anti-Mouse 647 (2 μg/mL, Jackson ImmunoResearch, 715-605-150), Donkey anti-Mouse 546 (2 μg/mL, Life Technologies, A10036), Donkey anti-Chicken 488 (2 μg/mL, Jackson ImmunoResearch, 703-545-155), Donkey anti-Goat 488 (2 μg/ml, Jackson ImmunoResearch, 705-545-147), Donkey anti-Rabbit Cy3 (2 μg/ml, Jackson ImmunoResearch, 711-165-152), Donkey anti-Rabbit 647 (2 μg/ml, Jackson ImmunoResearch, 711-605-152), and Donkey anti-Goat 647 (2 μg/mL, Invitrogen, A21447).

2.15. Flow Cytometry

OPCs were incubated with 3 μM CypHer-Aβ with 8 μg/ml clusterin, 1 μM CytoD, or a PBS vehicle control for 90 min. Cells were removed from the plate with 0.25 % Trypsin-EDTA (Gibco 25200056), washed, and stained with Ghost Dye Violet 510 (0.5 μL/test, Tonbo biosciences, 13–0870). Cells were analyzed using a 3 laser, 10-color Gallios flow cytometer (Beckman-Coulter).

2.16. Multiplex RNAscope (human)

Human tissue was embedded in paraffin and cut into 15 μM sections. Slices were heated for 48 h to allow attachment. Tissue was subsequently processed using the V2 RNAscope Fluorescent Multiplex Reagent Kit (Advanced Cell Diagnostics, 323100) according to manufacturer's instructions. Briefly, tissue was dehydrated using xylene and ethanol wash, treated with H_20_2, and then incubated in Target Retrieval Buffer at 95 °C for 15 min. Tissue was incubated with the supplied Protese Plus regent for 30 min. Target probes were hybridized to the tissue for 2 h at 40 °C, followed by hybridization of AMP1-FL (30 min, 40 °C), AMP2-FL (15 min, 40 °C), AMP3-FL

(30 min, 40 °C), and AMP4-FL (15 min, 40 °C). Tissue was then treated with an HRP reagent for a single probe, followed by a unique secondary, and an HRP blocker. This process was repeated for each probe used. Samples were counterstained with supplied DAPI or Hoechst 33342 (1:700, ThermoFisher Scientific, H3570) and mounted on slides using ProLong Glass Antifade Mountant (ThermoFisher, P36980). The following target probes were used: Human *OLIG2* (Advanced Cell Diagnostics, 424191-C2), Human *PDGFRA* (Advanced Cell Diagnostics, 604481), Human *CLU* (Advanced Cell Diagnostics, 584771-C3), and the RNAscope 4-plex Negative Control Probes (Advanced Cell Diagnostics, 321831). The following dyes were used: Opal 520 (Akoya Biosciences, FP1487001), Opal 690 (Akoya Biosciences, FP1497001), and Opal 620 (Akoya Biosciences, FP1495001). Sections were imaged using a Leica TCS SP8 confocal microscope.

2.17. Immunohistochemistry (human)

5 μm thick tissue sections of formalin fixed, paraffin embedded (FFPE) brain tissue specimens were rehydrated in Xylene and descending alcohol series and heat-induced epitope retrieval (HIER) was performed in a pressure cooker (Tintoretriever, Bio SB) for 15 min at high pressure in a 0.05 % Tween-20 solution. Endogenous peroxidase was quenched by incubation of sections in 1.5 % hydrogen peroxide/0.005 % Triton-X-100 diluted in pH 7.4 sterile phosphate buffered saline (PBS) (Invitrogen) for 20 min, following multiple washes in tap water and subsequently, 0.1 M Tris, pH 7.6. Non-specific antibody binding was minimized with sections incubated in 2 % FBS/0.1 M Tris, pH 7.6. Clusterin (Proteintech) primary antibody was diluted in 2 % FBS/0.1 M Tris, pH 7.6 at a dilution of 1:500. Sections were incubated with primary antibody over night at 4 °C, washed one time in 0.1 M Tris, pH 7.6, followed by 2 % FBS/0.1 M Tris, pH 7.6 for 5 min, incubated in goat ant-rabbit IgG HRP Conjugated secondary antibody (Millipore Sigma) for 1 h, additionally washed one time in 0.1 M Tris, pH 7.6, followed by 2 % FBS/0.1 M Tris, pH 7.6 for 5 min, and incubated in VectaStain ABC Peroxidase HRP Kit (diluted in 2 % FBS/0.1 M Tris, pH 7.6 at 1:1000) for 1 h. After a final wash in 0.1 M Tris, pH 7.6 for 5 min, immunocomplexes were visualized using the Vector Laboratories ImmPACT DAB Peroxidase (HRP) 3,3′-diaminobenzidine. Tissue sections were counterstained with hematoxylin (Sigma Aldrich, St. Louis, MO) for 2 min, dehydrated in ascending alcohol series and Xylene and cover slipped using Cytoseal 60 mounting medium (Thermo Scientific). For analysis of stains, slides of frontal cortex specimens stained with Clusterin antibodies were scanned on an Aperio AT2 scanner (Leica biosystems) at 20× magnification and digital slides analyzed using the QuPath platform (version 0.3.1, https://QuPath.github.io/, PMID: 29203879) on a Dell PC (Intel® Xeon® W-1270 CPU @ 3.40GHz/64 GB RAM/1 TB SSD Hard Drive) running Windows 10. Cortex and white matter were annotated for regional analysis. After exclusion of tissue and staining artifacts we used the 'Positive Pixel Detection' tool (Downsample factor 2, Gaussian sigma 1 μm, Hematoxylin threshold ('Negative') 1.5 OD units, DAB threshold ('Positive') 0.5 OD units) to determine the percentage of area covered by Clusterin staining.

2.18. Combined in situ hybridization and immunohistochemistry (human)

For in-situ hybridization, 5 μm thick paraffin-embedded tissue sections on slides were rehydrated in xylene and series of ethanol solutions (100 %, 90 %, and 70 %). Following air drying for 5 min at RT, slides were incubated with RNAscope® Hydrogen peroxide for 10 min at RT, followed by 3 washing steps in distilled water. Antigen retrieval was performed in a steam bath for 15 min using RNAscope® 1× target retrieval reagent. After a rinse in distilled water and incubation in 10 % ethanol for 3 min slides were air dried at 60 °C. Subsequently, slides were incubated with RNAscope® Protease plus reagent for 30 min at 40 °C in a HybEZ™ oven, followed by 3 washes in distilled water. Slides were then incubated with the following RNAscope® probe for 2 h at 40 °C in a HybEZ™ oven: Hs-Clusterin (cat. number 606241). Following washes with 1× Wash buffer, slides were incubated with RNAscope®AMP1 solution for 30 min at 40 °C. Subsequent incubations with other RNAscope® AMP solutions, followed each by two washes with 1× RNAscope® Wash buffer were completed as follows: AMP2 – 15 min at 40 °C; AMP3 – 30 min at 40 °C; AMP4 – 15 min at 40 °C; AMP5 – 30 min at RT and AMP6 – 15 min at RT. After two washes in 1× RNAscope® wash buffer slides were incubated in RNAscope® Fast RED-B and RED-A mixture (1:60 ratio) for 10 min at RT, followed by two washes in tap water. For in situ hybridization/immunohistochemistry double labeling, sections were incubated in 2 % FBS/0.1 M Tris, pH 7.6 for 5 min following RNAscope® Fast RED incubation and two washes in tap water. Primary antibodies were diluted in 2 % FBS/0.1 M Tris, pH 7.6 at the following dilutions: Ab5 (PMID: 16341263), 1:1000. Sections were incubated with primary antibody over night at 4 °C, washed two times in 0.1 M Tris, pH 7.6 for 5 min each and incubated with biotinylated secondary antibody (Vector Laboratories; Burlingame, CA) diluted in 2 % FBS/0.1 M Tris, pH 7.6 for 1 h at room temperature. An avidin-biotin complex (ABC) system (Vectastain ABC Elite kit; Vector Laboratories, Burlingame, CA) was used to enhance detection of the immunocomplexes, which were visualized using the chromogen 3,3′-diaminobenzidine (DAB kit; KPL, Gaithersburg, MD). Tissue sections were counterstained with hematoxylin (Sigma Aldrich, St. Louis, MO), air dried at 60 °C for 30 min and cover slipped using EcoMount™ mounting medium (Biocare Medical).

2.19. RT-qPCR

RNA was extracted from samples using the ISOLATE II RNA Micro Kit (Bioline, BIO-52075) or the ISOLATE II RNA Mini Kit (Bioline, BIO-52073). Isolated RNA was reverse transcribed using the SensiFAST cDNA Synthesis Kit (Bioline, BIO-65054) or the iScript cDNA Synthesis Kit (Bio-Rad, 1708891). RT-qPCR was performed using the SensiFAST Probe No-ROX Kit (Bioline, BIO-86005) and TaqMan probes for *Gapdh* (ThermoFisher, Mm99999915_g1), *Mbp* (ThermoFisher, Mm01266402_m1 and Mm01266403_m1), *Plp1* (ThermoFisher, Mm00456892_m1), *Cnp* (ThermoFisher, Mm01306641_m1), *Myrf* (ThermoFisher, Mm01194959_m1), and *Clu* (ThermoFisher, Mm00442773_m1). Additionally, the SensiFAST SYBR No-ROX Kit (Bioline, BIO-98005) was used with primers for *Plp1* (Forward:

GCCCCTACCAGACATCTAGC, Reverse: AGTCAGCCGCAAAACAGACT) and *Myrf* (CGGCGTCTCGACAGCCTCAA, Reverse: GACACGGCAAGAGAGCCGTCA). Data was collected using the CFX384 Real-Time System (Bio-rad).

2.20. Immunoblot

Cells were extracted in RIPA buffer containing a Protease Inhibitor Cocktail (Medchem Express). Lysates were centrifuged (13,000×*g*, 4 °C) for 15 min, and protein concentration was quantified using a BCA assay. After the addition of a protease inhibitor, conditioned media were concentrated using 10 kDa protein concentrators. Equal amounts of protein were loaded onto a Protean TGX gel (Bio-Rad) and transferred to a PVDF membrane. Membranes were blocked in 5 % milk in TBS-Tween 0.1 % for 1 h at room temperature. Primary antibody incubation was performed overnight at 4 °C. Washes were conducted in TBS-Tween 0.1 %, and membranes were incubated with secondary antibodies conjugated to HRP (Invitrogen) for 1 h at room temperature. The membranes

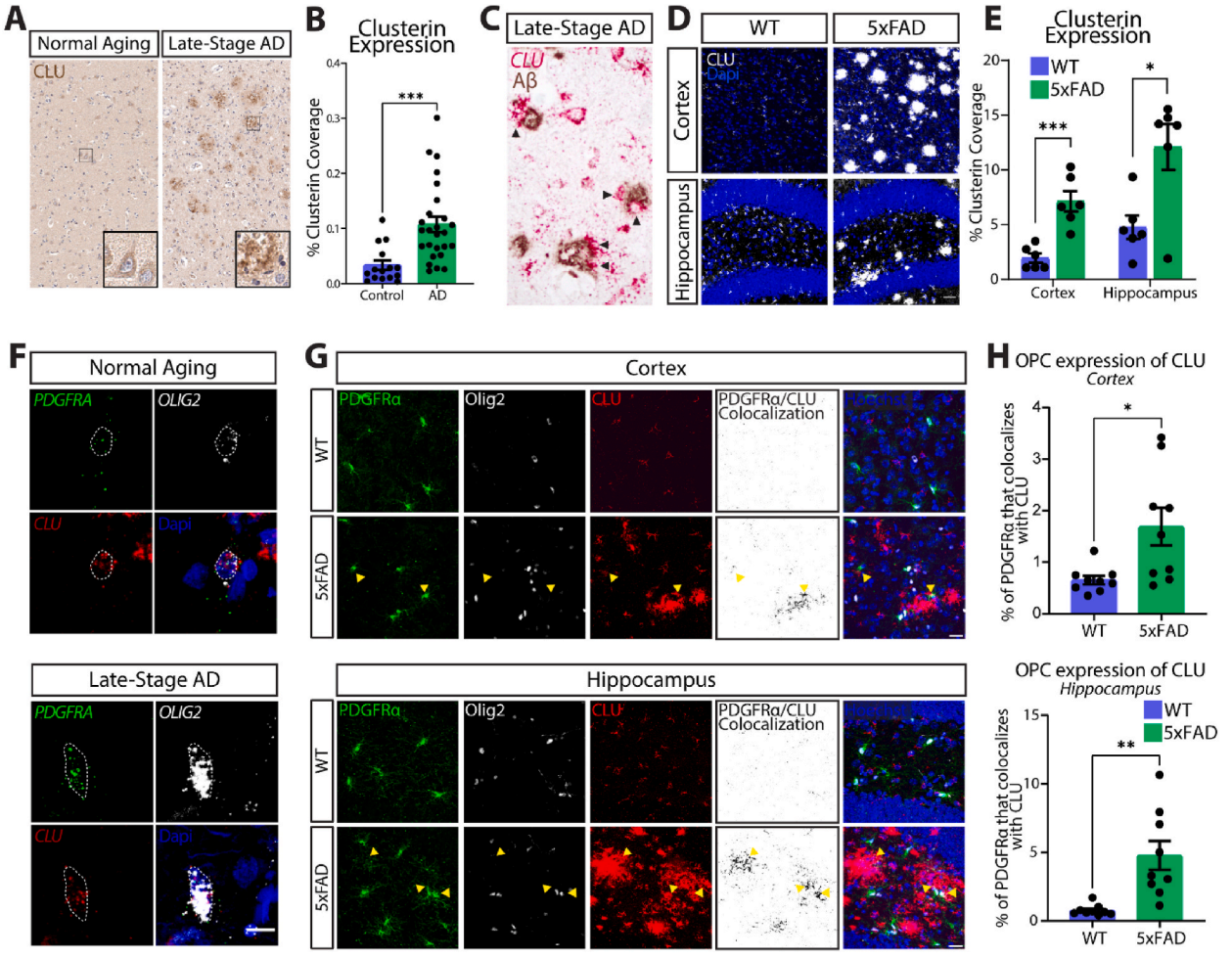

Fig. 1. OPCs express the AD-risk factor clusterin.
A, Representative image of Clusterin expression (immunohistochemistry, brown) in the cortex from a normal aging patient and a late-stage AD patient **B**, Quantification of clusterin coverage in the cortex of normal aging ($n = 15$) and AD patients ($n = 26$, from two independent experiments, depicted in **A**). Data analyzed using an unpaired *t*-test; t(39) = 3.767. **C**, Detection of clusterin RNA (in situ hybridization, red) and Aβ protein (immunohistochemistry, brown) in late-stage AD brain (late-stage AD $n = 2$; from two independent experiment). Arrowheads indicate clusterin-expressing cells around plaques. **D**, Representative images of clusterin expression (white) in the cortex and hippocampus of WT and 5xFAD mice. Scale bar = 30 μm. **E**, Quantification of clusterin coverage in the cortex and hippocampus of WT and 5xFAD mice (depicted in **C**; WT $n = 6$, 5xFAD $n = 6$; from two independent experiments). Statistics calculated using an unpaired Student's t-test. Cortex: t(10) = 5.049; Hippocampus: t (10) = 3.119. **F**, *In situ hybridization* for OPCs (*PDGFRA* in green, *OLIG2* in white) expressing Clusterin (*CLU*; red) in normal aging and late-stage AD brains (Dashed circles mark the nucleus, normal aging $n = 1$, late-stage AD $n = 1$; from one independent experiment). Scale bar = 10 μm. **G**, Representative images of clusterin expression (red) in OPCs (Pdgfrα; green and Olig2; white) in the cortex and hippocampus of WT and 5xFAD mice. Colocalization of Pdgfrα and clusterin depicted in black on a white background. Scale bar = 20 μm. **H**, quantification of the percentage of Pdgfrα that colocalizes with clusterin in the cortex and hippocampus of WT and 5xFAD mice (depicted in **G**; WT $n = 9$, 5xFAD $n = 9$; from two independent experiments). Statistics calculated using an unpaired Student's t-test. Cortex: t(16) = 2.761; Hippocampus: t(16) = 3.765.

were developed using Western Lightning Plus ECL (PerkinElmer). Densitometry was performed using Fiji.

2.21. Statistical analysis

Statistical analysis of all data was done using Prism 9 (Graphpad software). Significance was set at $p < 0.05$.

3. Results

3.1. Clusterin expression is increased in OPCs in 5xFAD mice and AD patients

Clusterin expression is elevated in the brains of patients with Alzheimer's disease (AD) and is a significant risk factor for development of late stage onset pathology [30]. Although clusterin production by astrocytes has been shown to influence neuronal functions in several contexts [12], clusterin expression has recently also been demonstrated in oligodendrocyte precursor cells (OPCs) through

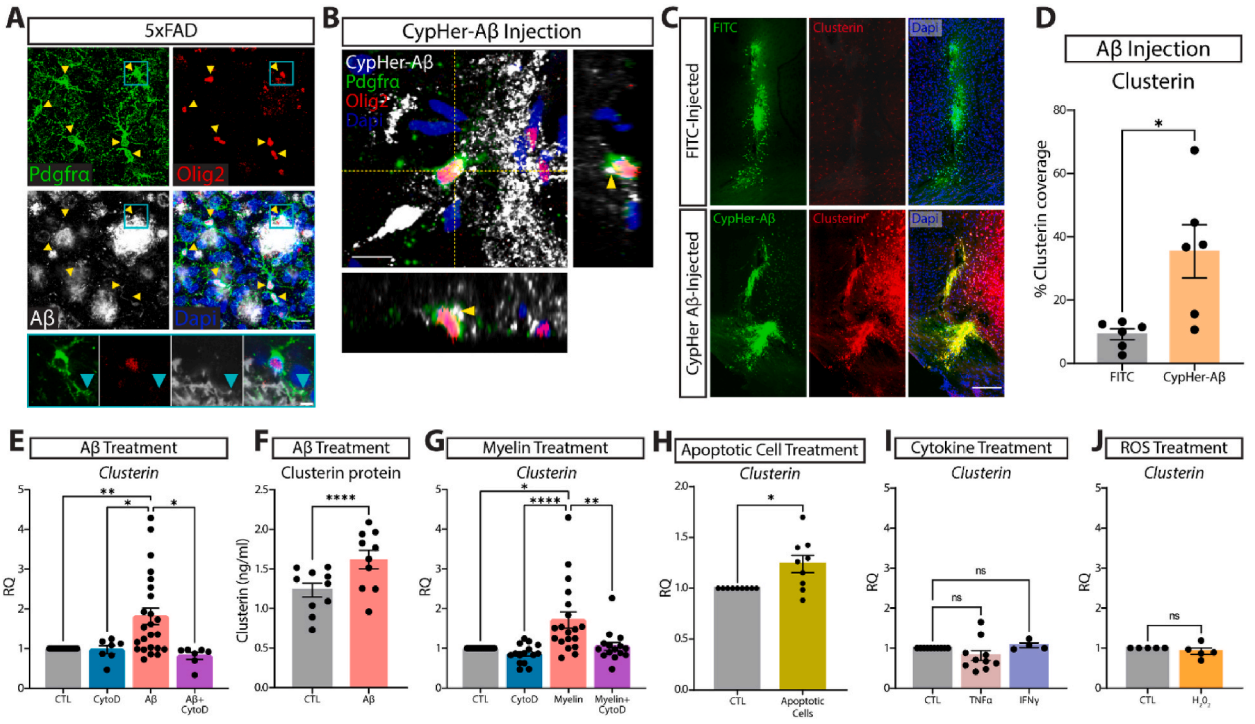

Fig. 2. Phagocytosis of extracellular debris drives clusterin expression in OPCs.
A, Representative image of OPCs (PDGFRα in green, Olig2 in red) surrounding Aβ plaques (white). Yellow arrowheads indicate OPCs that are extending processes into areas of Aβ accumulation. Inset is a single z-plane from main image. Teal arrow represents Aβ colocalizing with the process of a peri-plaque OPC ($n = 4$ mice; from one independent experiment). Scale bar = 20 μm for main image, 5 μm for inset. **B**, Representative orthogonal view of CyPher-labeled Aβ (white) inside an OPC (PDGFRα in green, Olig2 in red) following intra-parenchymal injection of Aβ ($n = 6$ mice; from one independent experiment). Yellow arrowheads indicate Aβ that can be seen inside the cell body of an OPC. Scale bar = 10 μm. **C**, Representative images of clusterin expression (red) in the ipsilateral (CypHer-Aβ injected; green) and contralateral (FITC injected; green) hemispheres following intra-parenchymal injection. Scale bar = 100 μm. **D**, Quantification of clusterin expression in the ipsilateral (Aβ-injected) and contralateral (FITC-injected) hemispheres following intra-parenchymal injection. ($n = 6$ mice). Statistics calculated using a paired Student's t-test; $t(5) = 2.979$. **E**, qPCR analysis of clusterin expression in OPCs following a 4-h *in vitro* treatment with 3 μm Aβ and the phagocytosis blocker CytoD (1 μm) or vehicle control (CTL $n = 24$, CytoD $n = 7$, Aβ $n = 24$, Aβ+CytoD $n = 7$; from seven independent experiments). Statistics calculated using a mixed effects analysis with a Tukey's post-hoc analysis; $F(1.121, 13.08) = 8.544$. **F**, Quantification by ELISA of clusterin protein in OPCs following 72-h treatment with 3 μM Aβ or vehicle control (CTL $n = 10$, Aβ $n = 10$, from two independent experiments). Statistics calculated using a paired Student's t-test; $t(9) = 7.596$. **G**, qPCR analysis of clusterin expression in OPCs following a 4-h *in vitro* treatment with 100 μg/ml myelin and CytoD (1 μm) or vehicle control (CTL $n = 19$, CytoD $n = 15$, Myelin $n = 19$, Myelin + CytoD $n = 15$; from five independent experiments). Statistics calculated using a mixed effects analysis with a Tukey's post-hoc analysis; $F(1.389, 21.29) = 10.75$. **H,** qPCR analysis of clusterin expression in OPCs following a 6-h *in vitro* treatment with apoptotic cells (CTL $n = 9$, Apoptotic cells $n = 9$; from two independent experiments). Statistics calculated using a paired Student's t-test; $t(8) = 2.835$. **I**, qPCR analysis of clusterin expression in OPCs following a 3-h *in vitro* treatment with 10 ng/ml TNFα or 10 ng/ml IFNγ (CTL $n = 10$, TNFα $n = 10$, IFNγ n = 4; from 2 independent TNFα experiments or 1 independent IFNγ experiment). Statistics calculated using a mixed effects analysis; $F(1.106, 11.61) = 1.897$. **J**, qPCR analysis of clusterin expression in OPCs following a 3-h *in vitro* treatment with 10 μm H_2O_2 ($n = 5$; from one independent experiment). Statistics calculated using a paired Student's t-test; $t(8) = 0.3417$. *$p < 0.05$, **$p < 0.01$, ****$p < 0.0001$, ns = not significant. All error bars represent SEM.

transcriptional analysis of both human and mouse brains [5,26]. Here, we investigated the regulation and function of clusterin in OPC myelination in the context of AD. We first confirmed that clusterin expression is increased in late-stage AD patients, compared to healthy aging controls (Fig. 1A and B). Using RNA in situ hybridization in combination with immunohistochemistry, we found that cells that express the *CLUSTERIN* transcript could be found directly surrounding the Aβ plaques (Fig. 1C). *Clusterin* is also elevated in multiple brain regions of 5xFAD mice, a pre-clinical model of AD, compared to healthy age-matched control mice (Fig. 1D and E). Because of the emerging role of OPCs and myelin in AD pathology, we investigated whether cells that express clusterin in AD could include OPCs [14,74]. Using RNAscope, we noted the *CLUSTERIN* transcript expression in OPCs during both normal aging and in AD pathology (Fig. 1F). We next detected the clusterin protein in healthy (WT) and AD-like 5xFAD mice and determined its co-localization with OPCs by immunofluorescence. Sections were stained with PDGFRα and OLIG2 (OPC markers) along with clusterin. To quantify clusterin signals specifically in OPCs and to exclude other cell types known to express clusterin, such as astrocytes—we extracted the overlap between the OPC marker PDGFRα and clusterin (black-and-white images in Fig. 1G). Consistent with our RNA-level findings, clusterin protein levels were elevated in AD-like pathology. We observed significantly increased co-localization of PDGFRα and clusterin in the cortex and hippocampus of 5xFAD mice compared to healthy controls (arrowheads, Fig. 1G and H).

Collectively, these data show that clusterin, a risk factor for late-onset AD, is upregulated in the parenchyma of AD patients in cells that are near the Aβ plaques, including OPCs, which can increase clusterin production AD-like conditions.

3.2. *Phagocytosis of oligomeric Aβ and cellular debris increases clusterin expression in OPC*

We next wanted to determine if OPCs could interact with Aβ plaques and contribute to AD pathology. We used immunofluorescence to detect Aβ and OPCs in the brain of 5xFAD mice, and we found OPCs adjacent to Aβ plaques, surrounding and extending their processes into the plaque areas (arrowheads, Fig. 2A). Because clusterin can facilitate clearance of particulate debris, we next wondered if OPCs were involved in engulfment of Aβ in the brain [71]. To test this, we injected healthy mice with Aβ oligomers labeled with CypHer5e, a pH-sensitive dye that fluoresces upon entering the acidic environment of the lysosome. Through Z-stack reconstruction of PDGFRα and OLIG2 co-localization with CypHer5e-Aβ oligomers, we found that OPCs around the injection site phagocytosed Aβ within 12 h of injection (Fig. 2B, Supplementary Fig. 1). It is important to note that Aβ oligomers were also detected away from the OPC markers, suggesting that they are likely internalized by other cells in the brain, in addition to the OPCs (Fig. 2B, Supplementary Fig. 1). Strikingly, Aβ injection led to robust increase in clusterin levels surrounding the injection site, which was not observed after injection of a FITC control (Fig. 2C and D). These data suggest that Aβ oligomers can elicit clusterin production.

We next investigated whether OPCs could contribute to this Aβ-induced upregulation of clusterin levels. We treated primary OPCs *in vitro* with Aβ oligomers for 4 h and measured *Clusterin* transcript expression by qRT-PCR. Exposure to Aβ oligomers significantly increased *Clusterin* transcript expression (Fig. 2E). Actin dependent phagocytosis of Aβ was necessary for clusterin upregulation, as treatment with cytochalasin D (CytoD), an actin polymerization inhibitor [3], prevented Aβ-induced *Clusterin* increase in OPCs (Fig. 2E). Because OPCs can uptake myelin and cellular debris [24], we tested whether phagocytosis of cellular contents can also increase clusterin expression. OPCs incubated with myelin were also upregulating *Clusterin* transcript in a phagocytosis-dependent manner inhibitable with cytoD (Fig. 2G). Similarly, OPCs incubated with apoptotic cells also increased clusterin expression (Fig. 2H). To test the possibility that this clusterin upregulation was simply a response to any cellular stressor, we treated OPCs with other factors known to be upregulated in Alzheimer's disease, including TNFα, IFNγ, and reactive oxygen species (ROS), none of which elevated clusterin expression (Fig. 2I and J) [8,10,72]. Finally, we tested whether clusterin protein levels in OPCs were increased after incubation with Aβ. Although clusterin protein levels were high in cultured OPCs, they were significantly increased after exposure to Aβ (Fig. 2F). We also tested the effect of Aβ oligomers on clusterin expression in another cell type. Expression of clusterin by Astrocytes, which are known to express clusterin [12], was not impacted after incubation with Aβ oligomers (Supplementary Figs. 2A and B).

Because treatment of phagocytes with clusterin can increase their phagocytic capacity in some contexts [4,67], we investigated whether extracellular clusterin may increase phagocytosis of Aβ by OPCs. However, adding exogenous clusterin during OPC phagocytosis of Aβ oligomers *in vitro* did not enhance their uptake (Fig. 3A and B).

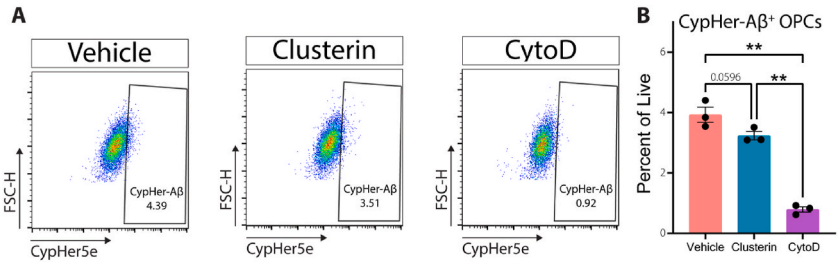

Fig. 3. Clusterin does not alter OPC phagocytosis of oligomeric Aβ.
A, Representative flow gating (following singlets/singlets/live gates) of OPCs incubated for 90 min with 3 μm CypHer5e-labeled Aβ oligomers (all conditions) with the addition of 8 μg/ml clusterin or 1 μm CytoD (Vehicle $n = 3$, Clusterin $n = 3$, CytoD $n = 3$; from one independent experiment). CypHer + gate was drawn so that less than 1 % of cells in the CytoD samples fell within the positive gate. **B**, Quantification of OPCs staining positive for CypHer-Aβ as depicted in **A**. Statistics calculated using a repeated measures one-way ANOVA with a Tukey's post-hoc analysis; $F(2,4) = 293.3$. $^{**}p < 0.01$. All error bars represent SEM.

Collectively, these data suggest that actin dependent uptake of Aβ oligomers and cellular debris increases clusterin production in OPCs, but clusterin does not subsequently regulate the phagocytosis of Aβ.

3.3. Exogenous clusterin inhibits OPC differentiation

Formation of new myelin is a critical component of memory function [49,57] and drugs that promote nascent myelin formation improve memory skills in a model of AD [14], highlighting the importance of understanding the factors that prevent differentiation of OPCs into myelinating oligodendrocytes. Cellular debris and protein aggregation can prevent OPC differentiation through yet unclear mechanisms [36,59]. This prompted us to ask whether clusterin could inhibit OPC differentiation. We treated OPCs with exogenous clusterin under conditions that facilitate differentiation into oligodendrocytes (OLG) and observed that treatment with clusterin decreases expression of genes that encode myelin proteins, such as *Mbp*, *Plp1*, and *Cnp*, as well as *Myrf*, the master transcriptional regulator of the OPC differentiation program (Fig. 4A–D). Subsequently, we observed fewer MBP-positive oligodendrocytes when OPCs were differentiated in the presence of clusterin, compared to vehicle (Fig. 4E and F). Importantly, OPC viability was not impacted by clusterin treatment (Fig. 4G). Overall, these data show that clusterin production is increased by phagocytosis of cellular debris and Aβ oligomers and that clusterin is a potent inhibitor of OPC differentiation.

3.4. Clusterin inhibits differentiation by reducing IL-9 production

We next investigated how clusterin mediates inhibition of OPC differentiation. OPCs produce a variety of growth factors, cytokines, and chemokines that modulate the local environment [7,34,38,44,55,56,65,75]. Therefore, we performed a Luminex Assay on the supernatants of OPCs treated with clusterin, compared to vehicle. We noted that clusterin treatment significantly elevates production of inflammatory chemokines CXCL1 and CXCL2, and the growth factor VEGF, while potently suppressing production of interleukin-9, or IL-9 (Fig. 5A). Since growth factors from the VEGF family have been shown to induce OPC proliferation [31], we first tested whether

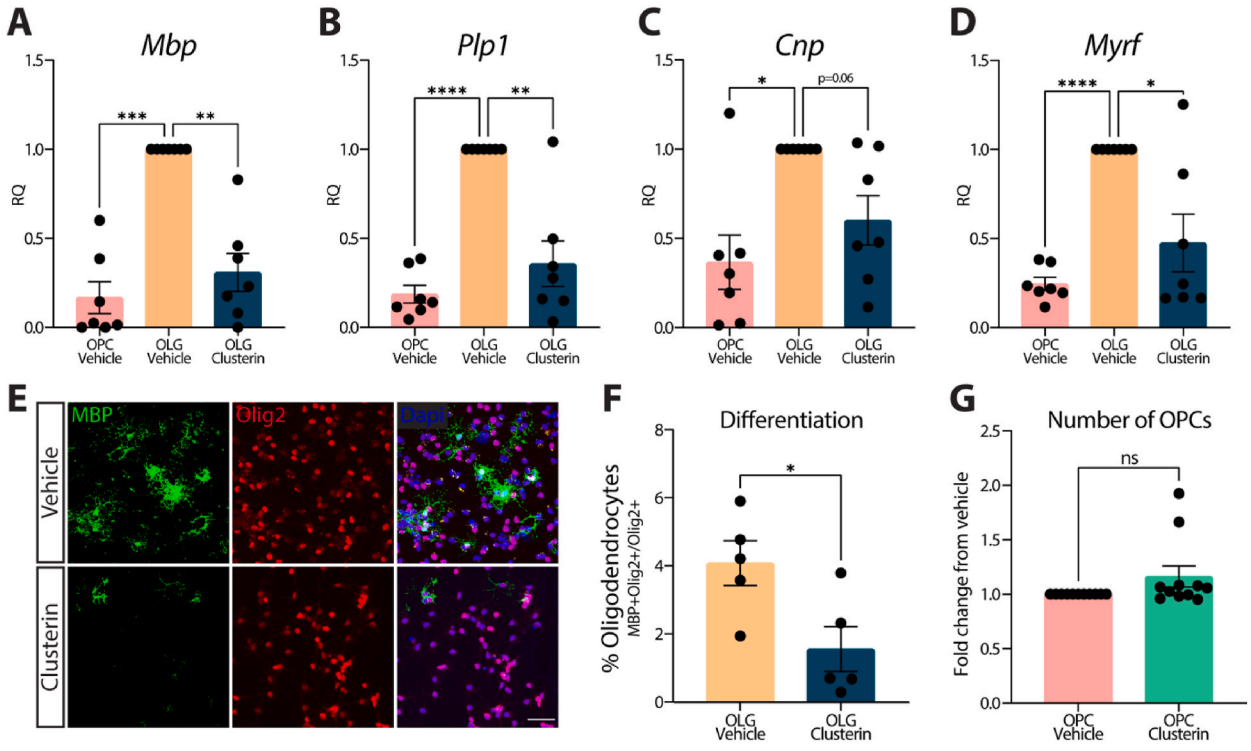

Fig. 4. Exogenous clusterin inhibits OPC differentiation.
Expression of *Mbp* (**A**), *Plp1* (**B**), *Cnp* (**C**), and *Myrf* (**D**), measured by qPCR in OPCs cultured in proliferation media (OPC Vehicle), differentiation media (OLG Vehicle), or differentiation media supplemented with 8 μg/ml of clusterin (OLG Clusterin) for 72 h ($n = 7$ for all conditions; from 3 independent experiments). Statistics calculated using a repeated measures one-way ANOVA with a Tukey's post-hoc analysis; *Mbp* $F(2,6) = 27.41$, *Plp1* $F(2,6) = 25.72$, *Cnp* $F(2,6) = 9.776$, *Myrf* $F(2,6) = 16.41$. **E**, Representative images of OPCs cultured in differentiation media with or without 8 μg/ml of clusterin for 72 h and stained for oligodendrocyte markers (MBP in green, Olig2 in red). Scale bar = 50 μm. **F**, Quantification of the number of OPCs that differentiated in to oligodendrocytes following treatment with clusterin (depicted in **E**; $n = 5$ for all conditions; from two independent experiments). Statistics calculated using a paired Student's t-test; $t(4) = 2.780$. **G**, Quantification of the number of OPCs present using a Cell Counting Kit-8 assay following a 72 h incubation in proliferation media with or without 8 μg/ml clusterin ($n = 11$ for all conditions; from four independent experiments). *$p < 0.05$, **$p < 0.01$, ****$p < 0.0001$, ns = not significant. All error bars represent SEM.

increased VEGF induced by clusterin treatment was responsible for keeping OPCs in an undifferentiated state. However, adding an anti-VEGF neutralizing antibody during the clusterin treatment of OPCs failed to rescue their differentiation (Supplementary Figs. 3A–C).

Since CXCR2 activating chemokines have been shown to influence OPC migration but not differentiation [63], we next tested the importance of IL-9, which was reduced by more than 90 % following clusterin treatment (Fig. 5A). IL-9 is a relatively understudied cytokine known to be produced mainly by T-cells to influence T cell and mast cell responses, but it's production and role in OPC differentiation have not been studied uncoupled from inflammatory triggers [21]. Surprisingly, we found that sole addition of exogenous IL-9 could rescue OPC differentiation in the presence of clusterin (Fig. 5B–D). Overall, these data demonstrate that clusterin likely blocks differentiation of OPCs at least partially by inhibiting the production of IL-9, as adding IL-9 is sufficient to overcome inhibition by clusterin.

3.5. *Clusterin deletion improves myelination in vivo*

Because clusterin inhibits OPC myelination *in vitro*, we next wanted to test if clusterin deletion would affect myelination *in vivo*. We obtained clusterin knockout mice [42], which are viable and fertile, and performed transmission electron microscopy (TEM) on the corpus callosum of 9-month-old clusterin knockout mice ($Clu^{-/-}$), compared to age-matched control mice. We measured the g-ratio of myelinated axons and found that $Clu^{-/-}$ mice had a lower g-ratio than control animals, indicating increased myelination (Fig. 6A and B). This result shows that, at baseline, clusterin expression has an inhibitory influence on myelination. Since clusterin expression increases in the 5xFAD model of AD, we next explored if deletion of clusterin could reverse myelination deficits observed in these mice [20,64,70]. To do this, we bred $Clu^{-/-}$ mice to 5xFAD mice to generate 5xFAD/$Clu^{-/-}$ mice. TEM measurement of the g-ratio of myelinated axons in the corpus callosum (9-month-old mice) again demonstrated decreased g-ratio of myelinated axons in the 5xFAD/$Clu^{-/-}$ mice, compared to the 5xFAD controls (Fig. 6C and D). Collectively, these results suggest that clusterin is a universal

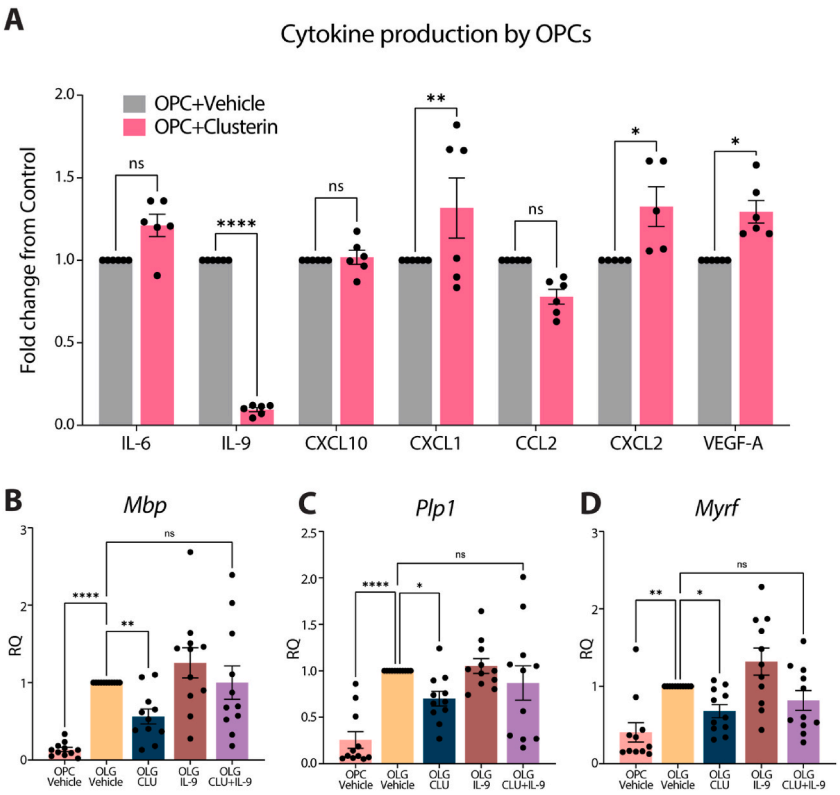

Fig. 5. Clusterin inhibits OPCs differentiation by blocking IL-9 production.
A, Quantification of cytokines present in the supernatant from OPCs treated with 8 μg/mL clusterin or vehicle control ($n = 6$ biological replicates for each condition, from two independent experiments). Data analyzed using a two-way repeated measures ANOVA with a Sidak's multiple comparison post-hoc analysis, $F(6, 34) = 23.93$. Expression of *Mbp* (**B**), *Plp1* (**C**), and *Myrf* (**D**), measured by qPCR in OPCs cultured in proliferation media (OPC Vehicle), differentiation media (OLG Vehicle), differentiation media supplemented with 8 μg/ml of clusterin (OLG CLU), differentiation media supplemented with 100 ng/ml IL-9 (OLG IL-9), or differentiation media supplemented with 8 μg/ml of clusterin and 100 ng/ml IL-9 (OLG CLU + IL-9) for 72 h ($n = 11$ for all conditions; from 3 independent experiments). Statistics calculated using a repeated measures one-way ANOVA with a Tukey's post-hoc analysis; *Mbp* $F(10,40) = 10.15$, *Plp1* $F(10,40) = 11.96$, *Myrf* $F(10,40) = 10.32$. *$p < 0.05$, **$p < 0.01$, ****$p < 0.0001$, ns = not significant. All error bars represent SEM.

inhibitor of myelination in homeostasis and AD-like pathology, and a potential target for treatment of myelin loss in neurodegeneration.

4. Discussion

Since the discovery of Aβ plaques in the brains of AD patients, therapeutic development has been focused on reducing plaque load. However, no therapeutic candidate, even when effective at reducing plaques, has succeeded in slowing down disease progression [32]. A growing body of literature speculates that other altered biological processes may be the driving force behind the clinical decline observed in AD patients [45]. Increasingly, OPCs and myelin are implicated in disease etiology and progression of AD symptoms. For example, ablation of senescent OPCs can reduce memory impairments observed in the APP/PS1 model of AD [74]. Additionally, inhibition of OPC differentiation prevents memory consolidation and recall, and therapeutic targeting to increase myelination improves memory performance in AD models [14,49,57,66]. Here, we offer a potential mechanism for the pervasive myelin deficits observed in Alzheimer's disease and the memory decline associated with these deficits [27,73]. We demonstrate that clusterin is upregulated in the brains of AD patients as well as in a mouse model of AD. We found that OPCs, alongside astrocytes [26], express clusterin during normal aging as well as in AD in humans and mice, and that OPCs increase production of the clusterin transcript and protein after exposure to Aβ oligomers. Further, we show that clusterin expression in OPCs is induced by actin dependent phagocytosis of debris, including Aβ oligomers, myelin, and apoptotic cells. Mechanistically, we discovered that clusterin mediates inhibition of OPC IL-9 secretion to block differentiation. Finally, clusterin deficiency *in vivo* results in thicker myelin sheath and prevents the myelin loss observed in 5xFAD mice.

SNPs in clusterin have been recognized as a significant risk factor for late onset AD for over a decade [6,28,37]. While there are conflicting reports in the literature regarding how this SNP effects the function and accumulation of clusterin, there is abundant evidence for high clusterin levels in the plasma (of AD patients) correlation with fastened cognitive decline and an increase in brain atrophy, even in the absence SNPs at the CLU locus [53,54,61,62]. These correlative studies demonstrate that excess levels of clusterin associate with increased severity of AD symptoms, and are supported by studies in mice, which show that clusterin deletion in mouse models of AD results in reduced plaque load and improved performance in memory tasks [19,48,68]. Importantly, however, there are also reports that suggest clusterin involvement in clearing Aβ plaques and protecting neurons [13,69]. These discrepancies likely indicate that the role of clusterin in regulation of neuronal homeostasis is complex and dependent on multiple factors, with detrimental effects likely observed when clusterin levels become supraphysiological in the context of disease pathology. Here, we uncover an additional piece of a puzzle in understanding the function of clusterin in AD, inhibition of OPC differentiation and myelination. Since

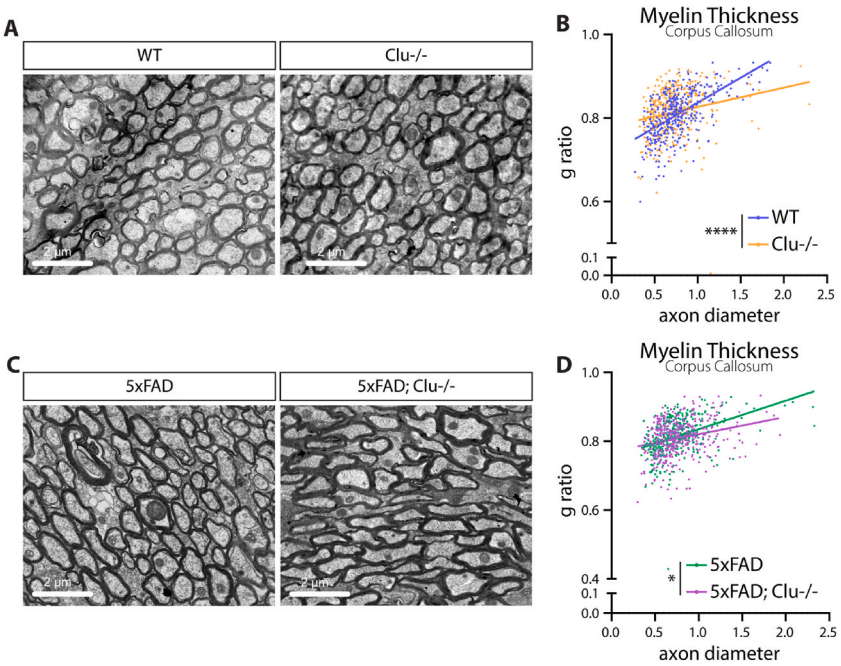

Fig. 6. Deletion of clusterin improves myelination in WT and 5XFAD mice.
A, Representative electron microscopy images of myelinated axons from the corpus callosum of 9-month old WT and clusterin knockout ($Clu^{-/-}$) mice. **B**, Quantification of the myelin g-ratio plotted against axon diameter in WT and Clu−/− mice. Lines represent linear regression of the plotted data and p-values represent comparison of slopes. **C**, Representative electron microscopy images of myelinated axons from the corpus callosum of 9-month old 5xFAD and 5xFAD; Clu−/− mice. **D**, Quantification of the myelin g-ratio plotted against axon diameter in 5xFAD and 5xFAD; Clu−/− mice. Lines represent linear regression of the plotted data and p-values represent comparison of slopes. *$p < 0.05$, ****$p < 0.0001$.

reduction of Aβ plaques in AD patients does not reliably improve clinical symptoms [1], we posit that the role of clusterin in inhibiting myelination may represent a viable therapeutic avenue for exploration in AD pathology.

We show here that deletion of clusterin *in vivo* increases myelination, which agrees with the finding that healthy human young adult carriers of one of the most common *CLUSTERIN* risk allele have reduced white matter integrity prior to the onset of cognitive decline [9], lending support to the concept that clusterin reduces the health of myelin tracts.

It remains to be determined which cell type(s) contribute the most to clusterin increase in Alzheimer's disease. While we have demonstrated that OPCs upregulate clusterin production in response to Aβ and cellular debris, and human single cell sequencing data show increase in clusterin expression in OPCs of AD patients, astrocytes have also been implicated as significant producers of clusterin [18,26]. Regardless of the cellular source, however, we hypothesize that extracellular clusterin profoundly impacts the function and differentiation capacity of OPCs.

It is now appreciated that OPCs contribute to cytokine production in several contexts, suggesting the potential for a broad immunomodulatory role of these cells [25,29,34,35,44,65]. Mechanistically, we show here that clusterin decreases OPC differentiation through suppression of IL-9 secretion. While IL-9 receptor expression in OPCs has been noted before [21], our report is the first to show that OPCs also produce IL-9, which critically promotes their differentiation.

Clusterin increase in the brains of AD patients has been appreciated for over three decades [40]. However, the mechanisms of clusterin's effects on the progression of AD remain unclear. Since the clusterin targeting antisense-oligonucleotide is already evaluated in clinical trials for the treatment of prostate cancer, our data shown here offer an exciting opportunity to explore the therapeutic efficacy of clusterin inhibition in improving myelin integrity and memory deficits in AD patients [15,16].

5. Conclusions

Collectively, we propose here a novel mechanism for the association between clusterin as a genetic risk factor and Alzheimer's disease myelin pathology, providing a foundation for development of therapeutic targeting of clusterin for the treatment of AD.

CRediT authorship contribution statement

Rebecca M. Beiter: Writing – review & editing, Writing – original draft, Methodology, Investigation, Formal analysis, Data curation, Conceptualization. **Tula P. Raghavan:** Methodology, Investigation, Formal analysis, Data curation. **Olivia Suchocki:** Methodology, Investigation. **Hannah E. Ennerfelt:** Investigation. **Courtney R. Rivet-Noor:** Investigation. **Andrea R. Merchak:** Investigation. **Jennifer L. Phillips:** Investigation. **Tim Bathe:** Investigation. **John R. Lukens:** Methodology. **Stefan Prokop:** Methodology, Investigation, Formal analysis. **Jeffrey L. Dupree:** Methodology, Investigation, Formal analysis. **Alban Gaultier:** Writing – review & editing, Writing – original draft, Supervision, Methodology, Investigation, Funding acquisition, Formal analysis, Conceptualization.

Availability of data and materials

The datasets and material generated during and/or analyzed during the current study are available from the corresponding author upon reasonable request.

Ethics approval

All animal experiments were approved and complied with regulations of the Institutional Animal Care and Use Committee at the University of Virginia (protocol #3918). All human tissue collection and preparation were approved by the Institutional Review Board at the University of Florida.

Declaration of competing interest

The authors declare that they have no known competing financial interests or personal relationships that could have appeared to influence the work reported in this paper.

Acknowledgements

The authors are supported by grants from the National Institutes of Health (RF1 AG079520, R21 AG083330, and R21 NS111204), Cure Alzheimer's fund, the Rick Sharp Alzheimer's Foundation, and the Owens Family Foundation. T.P.R is supported by T32 GM007267 and T32 GM148379. A.R.M. is supported by the T32 NS115657 and F31 AI174782. C.R.N is supported by the UVA Presidential Fellowship in Neuroscience.

Appendix A. Supplementary data

Supplementary data to this article can be found online at https://doi.org/10.1016/j.heliyon.2025.e41635.

References

[1] S.F. Ackley, S.C. Zimmerman, W.D. Brenowitz, E.J. Tchetgen Tchetgen, A.L. Gold, J.J. Manly, E.R. Mayeda, T.J. Filshtein, M.C. Power, F.M. Elahi, et al., Effect of reductions in amyloid levels on cognitive change in randomized trials: instrumental variable meta-analysis, BMJ (2021) n156, https://doi.org/10.1136/bmj.n156.

[2] Association As, 2021 Alzheimer's disease facts and figures, Alzheimer's Dementia 17 (2021) 327–406, https://doi.org/10.1002/alz.12328.

[3] S.G. Axline, E.P. Reaven, Inhibition of phagocytosis and plasma membrane mobility of the cultivated macrophage by cytochalasin B. Role of subplasmalemmal microfilaments, J. Cell Biol. 62 (1974) 647–659, https://doi.org/10.1083/jcb.62.3.647.

[4] M.M. Bartl, T. Luckenbach, O. Bergner, O. Ullrich, C. Koch-Brandt, Multiple receptors mediate apoJ-dependent clearance of cellular debris into nonprofessional phagocytes, Exp. Cell Res. 271 (2001) 130–141, https://doi.org/10.1006/excr.2001.5358.

[5] R.M. Beiter, C. Rivet-Noor, A.R. Merchak, R. Bai, D.M. Johanson, E. Slogar, K. Sol-Church, C.C. Overall, A. Gaultier, Evidence for oligodendrocyte progenitor cell heterogeneity in the adult mouse brain, Sci. Rep. 12 (2022) 12921, https://doi.org/10.1038/s41598-022-17081-7.

[6] C. Bellenguez, F. Kucukali, I.E. Jansen, L. Kleineidam, S. Moreno-Grau, N. Amin, A.C. Naj, R. Campos-Martin, B. Grenier-Boley, V. Andrade, et al., New insights into the genetic etiology of Alzheimer's disease and related dementias, Nat. Genet. 54 (2022) 412–436, https://doi.org/10.1038/s41588-022-01024-z.

[7] F. Birey, M. Kloc, M. Chavali, I. Hussein, M. Wilson, D.J. Christoffel, T. Chen, M.A. Frohman, J.K. Robinson, S.J. Russo, et al., Genetic and stress-induced loss of NG2 glia triggers emergence of depressive-like behaviors through reduced secretion of FGF2, Neuron 88 (2015) 941–956, https://doi.org/10.1016/j.neuron.2015.10.046.

[8] D.D. Bona, G. Candore, C. Franceschi, F. Licastro, G. Colonna-Romano, C. Cammà, D. Lio, C. Caruso, Systematic review by meta-analyses on the possible role of TNF-α polymorphisms in association with Alzheimer's disease, Brain Res. Rev. 61 (2009) 60–68, https://doi.org/10.1016/j.brainresrev.2009.05.001.

[9] M.N. Braskie, N. Jahanshad, J.L. Stein, M. Barysheva, K.L. McMahon, G.I. de Zubicaray, N.G. Martin, M.J. Wright, J.M. Ringman, A.W. Toga, et al., Common Alzheimer's disease risk variant within the CLU gene affects white matter microstructure in young adults, J. Neurosci. 31 (2011) 6764–6770, https://doi.org/10.1523/jneurosci.5794-10.2011.

[10] T.C. Browne, K. McQuillan, R.M. McManus, J.-A. O'Reilly, K.H.G. Mills, M.A. Lynch, IFN-Γ production by amyloid β–specific Th1 cells promotes microglial activation and increases plaque burden in a mouse model of Alzheimer's disease, J. Immunol. 190 (2013) 2241, https://doi.org/10.4049/jimmunol.1200947.

[11] H. Charkhkar, S. Meyyappan, E. Matveeva, J.R. Moll, D.G. McHail, N. Peixoto, R.O. Cliff, J.J. Pancrazio, Amyloid beta modulation of neuronal network activity in vitro, Brain Res. 1629 (2015) 1–9, https://doi.org/10.1016/j.brainres.2015.09.036.

[12] F. Chen, D.B. Swartzlander, A. Ghosh, J.D. Fryer, B. Wang, H. Zheng, Clusterin secreted from astrocyte promotes excitatory synaptic transmission and ameliorates Alzheimer's disease neuropathology, Mol. Neurodegener. 16 (2021) 5, https://doi.org/10.1186/s13024-021-00426-7.

[13] F. Chen, D.B. Swartzlander, A. Ghosh, J.D. Fryer, B. Wang, H. Zheng, Clusterin secreted from astrocyte promotes excitatory synaptic transmission and ameliorates Alzheimer's disease neuropathology, Mol. Neurodegener. 16 (2021), https://doi.org/10.1186/s13024-021-00426-7.

[14] J.-F. Chen, K. Liu, B. Hu, R.-R. Li, W. Xin, H. Chen, F. Wang, L. Chen, R.-X. Li, S.-Y. Ren, et al., Enhancing myelin renewal reverses cognitive dysfunction in a murine model of Alzheimer's disease, Neuron 109 (2021) 2292–2307.e2295, https://doi.org/10.1016/j.neuron.2021.05.012.

[15] K.N. Chi, E. Eisenhauer, L. Fazli, E.C. Jones, S.L. Goldenberg, J. Powers, D. Tu, M.E. Gleave, A phase I pharmacokinetic and pharmacodynamic study of OGX-011, a 2'-methoxyethyl antisense oligonucleotide to clusterin, in patients with localized prostate cancer, J. Natl. Cancer Inst. 97 (2005) 1287–1296, https://doi.org/10.1093/jnci/dji252.

[16] K.N. Chi, C.S. Higano, B. Blumenstein, J.-M. Ferrero, J. Reeves, S. Feyerabend, G. Gravis, A.S. Merseburger, A. Stenzl, A.M. Bergman, et al., Custirsen in combination with docetaxel and prednisone for patients with metastatic castration-resistant prostate cancer (SYNERGY trial): a phase 3, multicentre, open-label, randomised trial, Lancet Oncol. 18 (2017) 473–485, https://doi.org/10.1016/S1470-2045(17)30168-7.

[17] M.R. Dawson, A. Polito, J.M. Levine, R. Reynolds, NG2-expressing glial progenitor cells: an abundant and widespread population of cycling cells in the adult rat CNS, Mol. Cell. Neurosci. 24 (2003) 476–488.

[18] R.B. DeMattos, R.P. Brendza, J.E. Heuser, M. Kierson, J.R. Cirrito, J. Fryer, P.M. Sullivan, A.M. Fagan, X. Han, D.M. Holtzman, Purification and characterization of astrocyte-secreted apolipoprotein E and J-containing lipoproteins from wild-type and human apoE transgenic mice, Neurochem. Int. 39 (2001) 415–425, https://doi.org/10.1016/S0197-0186(01)00049-3.

[19] R.B. Demattos, M.A. O'Dell, M. Parsadanian, J.W. Taylor, J.A.K. Harmony, K.R. Bales, S.M. Paul, B.J. Aronow, D.M. Holtzman, Clusterin promotes amyloid plaque formation and is critical for neuritic toxicity in a mouse model of Alzheimer's disease, Proc. Natl. Acad. Sci. USA 99 (2002) 10843–10848, https://doi.org/10.1073/pnas.162228299.

[20] M.K. Desai, K.L. Sudol, M.C. Janelsins, M.A. Mastrangelo, M.E. Frazer, W.J. Bowers, Triple-transgenic Alzheimer's disease mice exhibit region-specific abnormalities in brain myelination patterns prior to appearance of amyloid and tau pathology, Glia 57 (2009) 54–65, https://doi.org/10.1002/glia.20734.

[21] X. Ding, F. Cao, L. Cui, B. Ciric, G.-X. Zhang, A. Rostami, IL-9 signaling affects central nervous system resident cells during inflammatory stimuli, Exp. Mol. Pathol. 99 (2015) 570–574, https://doi.org/10.1016/j.yexmp.2015.07.010.

[22] G. Falgarone, G. Chiocchia, Chapter 8: clusterin: A multifacet protein at the crossroad of inflammation and autoimmunity, Adv. Cancer Res. 104 (2009) 139–170, https://doi.org/10.1016/s0065-230x(09)04008-1.

[23] A. Fernandez-Castaneda, M.S. Chappell, D.A. Rosen, S.M. Seki, R.M. Beiter, D.M. Johanson, D. Liskey, E. Farber, S. Onengut-Gumuscu, C.C. Overall, et al., The active contribution of OPCs to neuroinflammation is mediated by LRP1, Acta Neuropathol. 139 (2020) 365–382, https://doi.org/10.1007/s00401-019-02073-1.

[24] A. Gaultier, X. Wu, N. Le Moan, S. Takimoto, G. Mukandala, K. Akassoglou, W.M. Campana, S.L. Gonias, Low-density lipoprotein receptor-related protein 1 is an essential receptor for myelin phagocytosis, J. Cell Sci. 122 (2009) 1155–1162, https://doi.org/10.1242/jcs.040717.

[25] R. Goswami, M.H. Kaplan, A brief history of IL-9, J. Immunol. 186 (2011) 3283–3288, https://doi.org/10.4049/jimmunol.1003049.

[26] A. Grubman, G. Chew, J.F. Ouyang, G. Sun, X.Y. Choo, C. McLean, R.K. Simmons, S. Buckberry, D.B. Vargas-Landin, D. Poppe, et al., A single-cell atlas of entorhinal cortex from individuals with Alzheimer's disease reveals cell-type-specific gene expression regulation, Nat. Neurosci. 22 (2019) 2087–2097, https://doi.org/10.1038/s41593-019-0539-4.

[27] X. Guo, Z. Wang, K. Li, Z. Li, Z. Qi, Z. Jin, L. Yao, K. Chen, Voxel-based assessment of gray and white matter volumes in Alzheimer's disease, Neurosci. Lett. 468 (2010) 146–150, https://doi.org/10.1016/j.neulet.2009.10.086.

[28] D. Harold, R. Abraham, P. Hollingworth, R. Sims, A. Gerrish, M.L. Hamshere, J.S. Pahwa, V. Moskvina, K. Dowzell, A. Williams, et al., Genome-wide association study identifies variants at CLU and PICALM associated with Alzheimer's disease, Nat. Genet. 41 (2009) 1088–1093, https://doi.org/10.1038/ng.440.

[29] E.P. Harrington, D.E. Bergles, P.A. Calabresi, Immune cell modulation of oligodendrocyte lineage cells, Neurosci. Lett. 715 (2020) 134601, https://doi.org/10.1016/j.neulet.2019.134601.

[30] S.K. Herring, H.-J. Moon, P. Rawal, A. Chhibber, L. Zhao, Brain clusterin protein isoforms and mitochondrial localization, Elife 8 (2019) e48255, https://doi.org/10.7554/eLife.48255.

[31] D. Hiratsuka, E. Kurganov, E. Furube, M. Morita, S. Miyata, VEGF- and PDGF-dependent proliferation of oligodendrocyte progenitor cells in the medulla oblongata after LPC-induced focal demyelination, J. Neuroimmunol. 332 (2019) 176–186, https://doi.org/10.1016/j.jneuroim.2019.04.016.

[32] C. Holmes, D. Boche, D. Wilkinson, G. Yadegarfar, V. Hopkins, A. Bayer, R.W. Jones, R. Bullock, S. Love, J.W. Neal, et al., Long-term effects of Aβ42 immunisation in Alzheimer's disease: follow-up of a randomised, placebo-controlled phase I trial, Lancet 372 (2008) 216–223, https://doi.org/10.1016/s0140-6736(08)61075-2.

[33] S.H. Kang, M. Fukaya, J.K. Yang, J.D. Rothstein, D.E. Bergles, NG2+ CNS glial progenitors remain committed to the oligodendrocyte lineage in postnatal life and following neurodegeneration, Neuron 68 (2010) 668–681, https://doi.org/10.1016/j.neuron.2010.09.009.

[34] Z. Kang, C. Wang, J. Zepp, L. Wu, K. Sun, J. Zhao, U. Chandrasekharan, P.E. DiCorleto, B.D. Trapp, R.M. Ransohoff, et al., Act1 mediates IL-17-induced EAE pathogenesis selectively in NG2+ glial cells, Nat. Neurosci. 16 (2013) 1401–1408, https://doi.org/10.1038/nn.3505.

[35] L. Kirby, G. Castelo-Branco, Crossing boundaries: interplay between the immune system and oligodendrocyte lineage cells, Semin. Cell Dev. Biol. 116 (2021) 45–52, https://doi.org/10.1016/j.semcdb.2020.10.013.

[36] M.R. Kotter, W.W. Li, C. Zhao, R.J. Franklin, Myelin impairs CNS remyelination by inhibiting oligodendrocyte precursor cell differentiation, J. Neurosci. 26 (2006) 328–332, https://doi.org/10.1523/JNEUROSCI.2615-05.2006.

[37] J.C. Lambert, S. Heath, G. Even, D. Campion, K. Sleegers, M. Hiltunen, O. Combarros, D. Zelenika, M.J. Bullido, B. Tavernier, et al., Genome-wide association study identifies variants at CLU and CR1 associated with Alzheimer's disease, Nat. Genet. 41 (2009) 1094–1099, https://doi.org/10.1038/ng.439.

[38] Y. Liang, N. Liang, Y. Ma, S. Tang, S. Ye, F. Xiao, Role of Clusterin/NF-κB in the secretion of senescence-associated secretory phenotype in Cr(VI)-induced premature senescent L-02 hepatocytes, Ecotoxicol. Environ. Saf. 219 (2021) 112343, https://doi.org/10.1016/j.ecoenv.2021.112343.

[39] S. Loveless, J.W. Neal, O.W. Howell, K.E. Harding, P. Sarkies, R. Evans, R.J. Bevan, S. Hakobyan, C.L. Harris, N.P. Robertson, et al., Tissue microarray methodology identifies complement pathway activation and dysregulation in progressive multiple sclerosis, Brain Pathol. 28 (2018) 507–520, https://doi.org/10.1111/bpa.12546.

[40] P.C. May, M. Lampert-Etchells, S.A. Johnson, J. Poirier, J.N. Masters, C.E. Finch, Dynamics of gene expression for a hippocampal glycoprotein elevated in Alzheimer's disease and in response to experimental lesions in rat, Neuron 5 (1990) 831–839, https://doi.org/10.1016/0896-6273(90)90342-d.

[41] I.A. McKenzie, D. Ohayon, H. Li, J.P. de Faria, B. Emery, K. Tohyama, W.D. Richardson, Motor skill learning requires active central myelination, Science 346 (2014) 318–322, https://doi.org/10.1126/science.1254960.

[42] L. McLaughlin, G. Zhu, M. Mistry, C. Ley-Ebert, W.D. Stuart, C.J. Florio, P.A. Groen, S.A. Witt, T.R. Kimball, D.P. Witte, et al., Apolipoprotein J/clusterin limits the severity of murine autoimmune myocarditis, J. Clin. Invest. 106 (2000) 1105–1113, https://doi.org/10.1172/JCI9037.

[43] H.J. Moon, S.K. Herring, L. Zhao, Clusterin: a multifaceted protein in the brain, Neural Regen Res 16 (2021) 1438–1439, https://doi.org/10.4103/1673-5374.301013.

[44] S. Moyon, A.L. Dubessy, M.S. Aigrot, M. Trotter, J.K. Huang, L. Dauphinot, M.C. Potier, C. Kerninon, S. Melik Parsadaniantz, R.J. Franklin, et al., Demyelination causes adult CNS progenitors to revert to an immature state and express immune cues that support their migration, J. Neurosci. 35 (2015) 4–20, https://doi.org/10.1523/JNEUROSCI.0849-14.2015.

[45] K. Mullane, M. Williams, Alzheimer's disease beyond amyloid: can the repetitive failures of amyloid-targeted therapeutics inform future approaches to dementia drug discovery? Biochem. Pharmacol. 177 (2020) 113945 https://doi.org/10.1016/j.bcp.2020.113945.

[46] N. Murphy, B. Grehan, M.A. Lynch, Glial uptake of amyloid beta induces NLRP3 inflammasome formation via cathepsin-dependent degradation of NLRP10, NeuroMolecular Med. 16 (2014) 205–215, https://doi.org/10.1007/s12017-013-8274-6.

[47] H. Oakley, S.L. Cole, S. Logan, E. Maus, P. Shao, J. Craft, A. Guillozet-Bongaarts, M. Ohno, J. Disterhoft, L. Van Eldik, et al., Intraneuronal beta-amyloid aggregates, neurodegeneration, and neuron loss in transgenic mice with five familial Alzheimer's disease mutations: potential factors in amyloid plaque formation, J. Neurosci. 26 (2006) 10129–10140, https://doi.org/10.1523/jneurosci.1202-06.2006.

[48] S.-B. Oh, M.S. Kim, S. Park, H. Son, S.-Y. Kim, M.-S. Kim, D.-G. Jo, E. Tak, J.-Y. Lee, Clusterin contributes to early stage of Alzheimer's disease pathogenesis, Brain Pathol. 29 (2019) 217–231, https://doi.org/10.1111/bpa.12660.

[49] S. Pan, S.R. Mayoral, H.S. Choi, J.R. Chan, M.A. Kheirbek, Preservation of a remote fear memory requires new myelin formation, Nat. Neurosci. 23 (2020) 487–499, https://doi.org/10.1038/s41593-019-0582-1.

[50] C.E. Pedraza, R. Monk, J. Lei, Q. Hao, W.B. Macklin, Production, characterization, and efficient transfection of highly pure oligodendrocyte precursor cultures from mouse embryonic neural progenitors, Glia 56 (2008) 1339–1352, https://doi.org/10.1002/glia.20702.

[51] J.V. Pluvinage, M.S. Haney, B.A.H. Smith, J. Sun, T. Iram, L. Bonanno, L. Li, D.P. Lee, D.W. Morgens, A.C. Yang, et al., CD22 blockade restores homeostatic microglial phagocytosis in ageing brains, Nature 568 (2019) 187–192, https://doi.org/10.1038/s41586-019-1088-4.

[52] A.E. Roher, N. Weiss, T.A. Kokjohn, Y.-M. Kuo, W. Kalback, J. Anthony, D. Watson, D.C. Luehrs, L. Sue, D. Walker, et al., Increased Aβ peptides and reduced cholesterol and myelin proteins characterize white matter degeneration in Alzheimer's disease, Biochemistry 41 (2002) 11080–11090, https://doi.org/10.1021/bi026173d.

[53] E.M. Schrijvers, P.J. Koudstaal, A. Hofman, M.M. Breteler, Plasma clusterin and the risk of Alzheimer disease, JAMA 305 (2011) 1322–1326, https://doi.org/10.1001/jama.2011.381.

[54] Schürmann B Association of the Alzheimer's disease clusterin risk allele with plasma clusterin concentration. J. Alzheim. Dis. 25: 421-424.

[55] Y.-J. Shim, B.-H. Kang, B.-K. Choi, I.-S. Park, B.-H. Min, Clusterin induces the secretion of TNF-α and the chemotactic migration of macrophages, Biochem Bioph Res Co 422 (2012) 200–205, https://doi.org/10.1016/j.bbrc.2012.04.162.

[56] Y.J. Shim, B.H. Kang, H.S. Jeon, I.S. Park, K.U. Lee, I.K. Lee, G.H. Park, K.M. Lee, P. Schedin, B.H. Min, Clusterin induces matrix metalloproteinase-9 expression via ERK1/2 and PI3K/Akt/NF-κB pathways in monocytes/macrophages, J. Leukoc. Biol. 90 (2011) 761–769, https://doi.org/10.1189/jlb.0311110.

[57] P.E. Steadman, F. Xia, M. Ahmed, A.J. Mocle, A.R.A. Penning, A.C. Geraghty, H.W. Steenland, M. Monje, S.A. Josselyn, P.W. Frankland, Disruption of oligodendrogenesis impairs memory consolidation in adult mice, Neuron 105 (2020) 150–164.e156, https://doi.org/10.1016/j.neuron.2019.10.013.

[58] W.B. Stine, L. Jungbauer, C. Yu, M.J. LaDu, Preparing synthetic Aβ in different aggregation states, in: E.D. Roberson (Ed.), Alzheimer's Disease and Frontotemporal Dementia: Methods and Protocols, Humana Press, City, 2011, pp. 13–32.

[59] J.M.J. Stoffels, J.C. de Jonge, M. Stancic, A. Nomden, M.E. van Strien, D. Ma, Z. Šišková, O. Maier, C. ffrench-Constant, R.J.M. Franklin, et al., Fibronectin aggregation in multiple sclerosis lesions impairs remyelination, Brain 136 (2013) 116–131, https://doi.org/10.1093/brain/aws313.

[60] D. Tanokashira, N. Mamada, F. Yamamoto, K. Taniguchi, A. Tamaoka, M.K. Lakshmana, W. Araki, The neurotoxicity of amyloid β-protein oligomers is reversible in a primary neuron model, Mol. Brain 10 (2017) 4, https://doi.org/10.1186/s13041-016-0284-5.

[61] M. Thambisetty, Y. An, A. Kinsey, D. Koka, M. Saleem, A. Güntert, M. Kraut, L. Ferrucci, C. Davatzikos, S. Lovestone, et al., Plasma clusterin concentration is associated with longitudinal brain atrophy in mild cognitive impairment, Neuroimage 59 (2012) 212–217, https://doi.org/10.1016/j.neuroimage.2011.07.056.

[62] M. Thambisetty, A. Simmons, L. Velayudhan, A. Hye, J. Campbell, Y. Zhang, L.O. Wahlund, E. Westman, A. Kinsey, A. Güntert, et al., Association of plasma clusterin concentration with severity, pathology, and progression in Alzheimer disease, Arch. Gen. Psychiatr. 67 (2010) 739–748, https://doi.org/10.1001/archgenpsychiatry.2010.78.

[63] H.H. Tsai, E. Frost, V. To, S. Robinson, C. Ffrench-Constant, R. Geertman, R.M. Ransohoff, R.H. Miller, The chemokine receptor CXCR2 controls positioning of oligodendrocyte precursors in developing spinal cord by arresting their migration, Cell 110 (2002) 373–383, https://doi.org/10.1016/s0092-8674(02)00838-3.

[64] I. Vanzulli, M. Papanikolaou, I.C. De-La-Rocha, F. Pieropan, A.D. Rivera, D. Gomez-Nicola, A. Verkhratsky, J.J. Rodríguez, A.M. Butt, Disruption of oligodendrocyte progenitor cells is an early sign of pathology in the triple transgenic mouse model of Alzheimer's disease, Neurobiol. Aging 94 (2020) 130–139, https://doi.org/10.1016/j.neurobiolaging.2020.05.016.

[65] C. Wang, C.-J. Zhang, B.N. Martin, K. Bulek, Z. Kang, J. Zhao, G. Bian, J.A. Carman, J. Gao, A. Dongre, et al., IL-17 induced NOTCH1 activation in oligodendrocyte progenitor cells enhances proliferation and inflammatory gene expression, Nat. Commun. 8 (2017) 15508, https://doi.org/10.1038/ncomms15508.

[66] F. Wang, S.-Y. Ren, J.-F. Chen, K. Liu, R.-X. Li, Z.-F. Li, B. Hu, J.-Q. Niu, L. Xiao, J.R. Chan, et al., Myelin degeneration and diminished myelin renewal contribute to age-related deficits in memory, Nat. Neurosci. 23 (2020) 481–486, https://doi.org/10.1038/s41593-020-0588-8.

[67] X. Weng, H. Zhao, Q. Guan, G. Shi, S. Feng, M.E. Gleave, C.C.Y. Nguan, C. Du, Clusterin regulates macrophage expansion, polarization and phagocytic activity in response to inflammation in the kidneys, Immunol. Cell Biol. 99 (2021) 274–287, https://doi.org/10.1111/imcb.12405.

[68] A.M. Wojtas, S.S. Kang, B.M. Olley, M. Gatherer, M. Shinohara, P.A. Lozano, C.-C. Liu, A. Kurti, K.E. Baker, D.W. Dickson, et al., Loss of clusterin shifts amyloid deposition to the cerebrovasculature via disruption of perivascular drainage pathways, Proc. Natl. Acad. Sci. USA 114 (2017) E6962–E6971, https://doi.org/10.1073/pnas.1701137114.

[69] A.M. Wojtas, J.P. Sens, S.S. Kang, K.E. Baker, T.J. Berry, A. Kurti, L. Daughrity, K.R. Jansen-West, D.W. Dickson, L. Petrucelli, et al., Astrocyte-derived clusterin suppresses amyloid formation in vivo, Mol. Neurodegener. 15 (2020), https://doi.org/10.1186/s13024-020-00416-1.

[70] D. Wu, X. Tang, L.H. Gu, X.L. Li, X.Y. Qi, F. Bai, X.C. Chen, J.Z. Wang, Q.G. Ren, Z.J. Zhang, LINGO-1 antibody ameliorates myelin impairment and spatial memory deficits in the early stage of 5XFAD mice, CNS Neurosci. Ther. 24 (2018) 381–393, https://doi.org/10.1111/cns.12809.

[71] A.R. Wyatt, J.J. Yerbury, P. Berghofer, I. Greguric, A. Katsifis, C.M. Dobson, M.R. Wilson, Clusterin facilitates in vivo clearance of extracellular misfolded proteins, Cell. Mol. Life Sci. 68 (2011) 3919–3931, https://doi.org/10.1007/s00018-011-0684-8.

[72] J. Yang, X. Zhang, P. Yuan, J. Yang, Y. Xu, J. Grutzendler, Y. Shao, A. Moore, C. Ran, Oxalate-curcumin–based probe for micro- and macroimaging of reactive oxygen species in Alzheimer's disease, Proc. Natl. Acad. Sci. USA 114 (2017) 12384, https://doi.org/10.1073/pnas.1706248114.
[73] X. Zhan, C. Jickling Gc, P. Ander B, D. Liu, B. Stamova, C. Cox, L.W. Jin, C. DeCarli, F. R Sharp, Myelin injury and degraded myelin vesicles in Alzheimer's disease, Curr. Alzheimer Res. 11 (2014) 232–238.
[74] P. Zhang, Y. Kishimoto, I. Grammatikakis, K. Gottimukkala, R.G. Cutler, S. Zhang, K. Abdelmohsen, V.A. Bohr, J. Misra Sen, M. Gorospe, et al., Senolytic therapy alleviates Aβ-associated oligodendrocyte progenitor cell senescence and cognitive deficits in an Alzheimer's disease model, Nat. Neurosci. (2019), https://doi.org/10.1038/s41593-019-0372-9.
[75] Y.W. Zhang, J. Denham, R.S. Thies, Oligodendrocyte progenitor cells derived from human embryonic stem cells express neurotrophic factors, Stem Cells Dev 15 (2006) 943–952, https://doi.org/10.1089/scd.2006.15.943.